Environmental Research Letters

LETTER • OPEN ACCESS

Assessment of hydrologic connectivity in an ungauged wetland with InSAR observations

To cite this article: Fernando Jaramillo *et al* 2018 *Environ. Res. Lett.* **13** 024003

IOP Publishing Environ. Res. Lett. 13 (2018) 024003 https://doi.org/10.1088/1748-9326/aa9d23

Environmental Research Letters

LETTER

RECEIVED
4 July 2017

REVISED
23 November 2017

ACCEPTED FOR PUBLICATION
24 November 2017

PUBLISHED
24 January 2018

Assessment of hydrologic connectivity in an ungauged wetland with InSAR observations

Fernando Jaramillo[1,2,3,8], Ian Brown[1], Pascal Castellazzi[4], Luisa Espinosa[5], Alice Guittard[1], Sang-Hoon Hong[6], Victor H Rivera-Monroy[7] and Shimon Wdowinski[1]

1 Department of Earth and Environment, Florida International University, Modesto Maidique Campus, AHC5, Room 375, Miami, FL, United States of America
2 Department of Physical Geography and Bert Bolin Centre for Climate Research, Stockholm University, SE–106 91, Stockholm, Sweden
3 Stockholm Resilience Centre, Stockholm University, SE–106 91, Stockholm, Sweden
4 Institut National de la Recherche Scientifique, Quebec City, Canada
5 Instituto de Investigaciones Marinas y Costeras 'José Benito Vives de Andreis'- INVEMAR, Cl. 25 #2– 55, Santa Marta, Magdalena, Colombia
6 Korea Polar Research Institute, Yeonsu-gu, Incheon, 406–840, Republic of Korea
7 Department of Oceanography and Coastal Sciences, College of the Coast and Environment, Louisiana State University, Baton Rouge, LA 70803, United States of America
8 Author to whom any correspondence should be addressed.

E-mail: fernando.jaramillo@natgeo.su.se

Keywords: wetland, hydrologic connectivity, InSAR, mangroves, freshwater input

Supplementary material for this article is available online

Abstract

The Ciénaga Grande de Santa Marta (CGSM) is one of the world's most productive tropical wetlands and one that has witnessed some of the greatest recorded dieback of mangroves. Human-driven loss of hydrologic connectivity by roads, artificial channels and water flow regulation appears to be the reason behind mangrove mortality in this ungauged wetland. In this study, we determined the CGSM's current state of hydrologic connectivity by combining a remote sensing technique, termed as Wetland Interferometric Synthetic Aperture Radar (InSAR), with a hydrologic study of river water discharge. For this research, we processed 29 ALOS-PALSAR acquisitions taken during the period 2007–2011 and generated 66 interferograms that provide information on relative surface water level changes. We found that change in water discharge upstream on the main tributary of the CGSM could explain at most 17% of the variance of the change in water level in the CGSM. Fresh water inputs into the wetland were identified only when the mean daily water discharge in the river exceeded 700 m^3 s^{-1}, which corresponds to only 30% of the days during the period. The interferogram analysis also revealed that artificial channels within the wetland serve as barriers to water flow and contribute to the overall loss in hydrologic connectivity. We recommend increasing fresh water inputs from the Magdalena River by reducing water regulation of fresh water from the river and improving connectivity on either side of the artificial channels crossing the CGSM. This study emphasizes the potential of the application of wetland InSAR to determine hydrologic connectivity in wetlands that are completely or poorly ungauged and to define the necessary guidelines for wetland hydrologic restoration.

1. Introduction

Wetland hydrologic connectivity refers to the transfer of matter, energy, or organisms within or between wetland elements or their hydrologic fluxes (Pringle 2001, Foti *et al* 2012). The hydrologic fluxes include multiple water transport pathways such as surface run-off, groundwater, and shallow subsurface flow at various scales (Golden *et al* 2014, Cohen *et al* 2016). Assessments of hydrologic connectivity are necessary to understand water flow and hydrologic transport of sediments and other pollutants in wetland ecosystems. They also provide the knowledge on wetland functions required to develop the studies of environmental

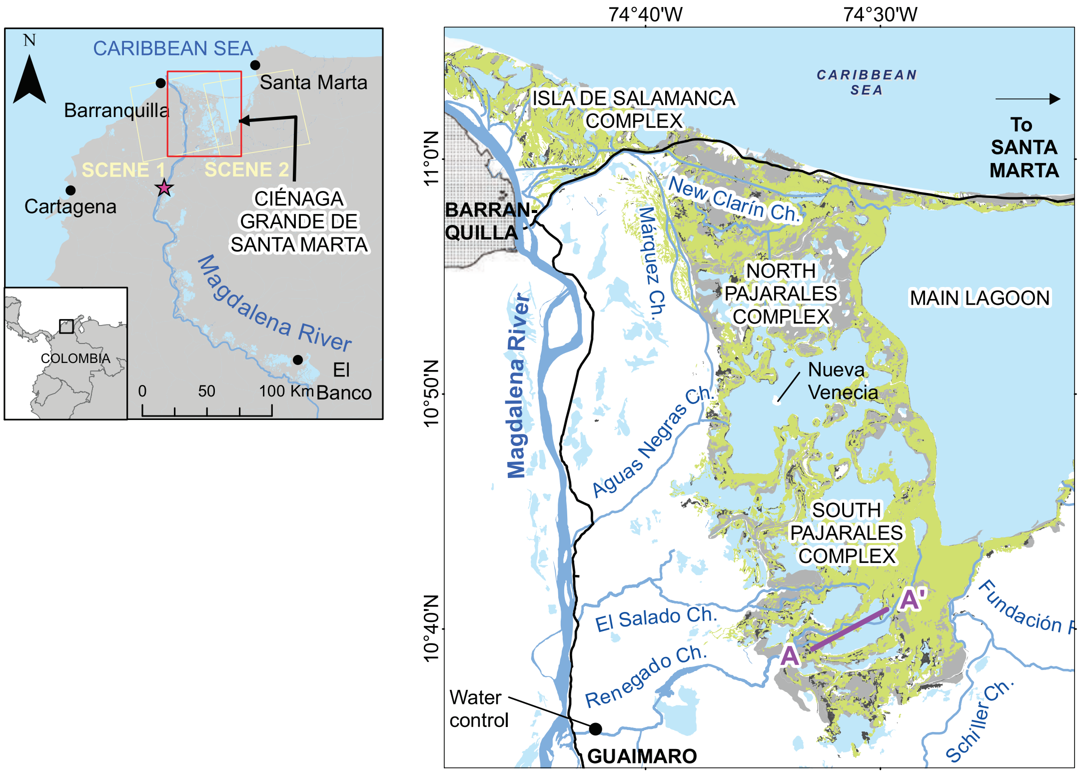

Figure 1. The Ciénaga Grande de Santa Marta wetland (CGSM). (*a*) Location of the CGSM on the Colombian Caribbean Coast and specific location of the Calamar discharge station on the Magdalena River (star). Yellow polygons depict the spatial coverage of the two scenes for which 29 acquisitions were collected (16 for Scene 1 and 13 for Scene 2). (*b*) Zoom (red in (*a*)) of the CGSM along with main channels of fresh water input from the Magdalena River (blue), and the two main roads (black) interrupting the flow of water between CGSM, river and sea. The road between Barranquilla and Santa Marta was initially constructed in the 1950's without adequate drainage systems, leading to the hydrologic isolation of the CGSM from the sea. The secondary road from Barranquilla to Guaimaro was constructed in the 1970's, restricting fresh water inputs from the Magdalena River. The Renegado channel is controlled at its mouth by a sluice gate for agricultural purposes. Mangrove coverage in 2016 is shown in green with dead mangrove areas that have not recovered to date represented in grey. Location of example transect of figure 2 is shown in purple.

impact, restoration and conservation (Freeman *et al* 2007, Quin *et al* 2015, Van Meter and Basu 2015, Thorslund *et al* 2017). Alteration in wetland connectivity is one of the major causes of wetland degradation globally (Jimenez *et al* 1985) and combined with macroclimatic changes, it can pose a highly detrimental threat to these ecosystems (Blanco *et al* 2006, Osland *et al* 2016). In the case of estuarine and coastal wetlands, such a combination has resulted in massive mortality episodes for mangroves (Barreto 2008, Cardona and Botero 1998, Cintron *et al* 1978). This is a cause for concern, since mangrove ecosystems are highly productive ecosystems, providing at least US $1.6 billion/year through ecosystem services and further support global coastal livelihoods (Polidoro *et al* 2010). The activities that are known to alter coastal wetland connectivity include flow regulation and consumption of water for agricultural purposes, road infrastructure, and urbanization, through reduction and even blockage of fresh water inputs into estuarine wetlands (Wemple *et al* 2017, Jaramillo and Destouni 2015).

The CGSM in Colombia presents an iconic case of alteration in wetland connectivity. This 1280 km^2 estuarine wetland complex forms the delta of the Magdalena River, the longest river in Colombia (figure 1) and is located between the two coastal cities of Barranquilla and Santa Marta. Over the last six decades, the wetland has experienced extended hydrologic modification through the construction of roads, artificial channels, and water flow regulation that have served to increase its vulnerability in relation to dry events of the El Niño-Southern Oscillation (Blanco *et al* 2006). These events augment surface water and pore water salinities resulting in prolonged hypersalinity conditions. Similar to many other areas in the world, hyper-salinity appears to be the main cause behind the CGSM's mangrove ecosystem's degradation and a significant controlling factor for mangrove development and rehabilitation (Botero and Salzwedel 1999, Cardona and Botero 1998, Rivera-Monroy *et al* 2011). From a historical mangrove coverage of 500 km^2, mangrove coverage in the CGSM had been reduced to only 226 km^2 in 1996 (INVEMAR 2016). Previous studies reveal that the exposure to high salinity levels affects early mangrove seedling establishment, growth, eco-physiological proficiency and can further lead to biochemical function impairment and mortality (Flowers and Yeo 1986, Krauss *et al* 2008).

Since 1996 coverage has recovered to 400 km^2, but has recently become stagnant (INVEMAR 2016). The recovery is attributed to a rehabilitation program implemented between 1994 and 1998 to reestablish the hydrologic connectivity of the wetland. The program consisted in dredging five pre-existing channels connecting the CGSM with the Magdalena River (Botero and Salzwedel 1999) and improving drainage under the two roads that had decreased hydrologic connectivity between the wetland, its main tributary and the sea (figure 1). The program estimated that a total water flow of 163 $m^3 s^{-1}$ (i.e. 2% of the mean annual discharge on the Magdalena River at its outlet into the Caribbean Sea) was the supply of fresh water needed to restore the wetland's mangrove ecosystems (Botero and Salzwedel 1999). After 2006, continued heavy siltation of material and channel clogging have necessitated additional dredging of 2.6×10^6 m^3 (Martínez 2005). Mangrove recovery has failed in several areas, implying that fresh water inputs are still too low and hyper-salinity continues.

The main objective of this investigation is to assess and quantify the current state of hydrologic connectivity within the CGSM and between the CGSM and its main tributary river. This will be accomplished with the knowledge that the roads, channel siltation, water flow regulation and hydrologic modifications restrict fresh water inputs and overall connectivity. Thus, we aim to identify the channels that currently control fresh water inputs into CGSM and the hydrologic conditions that enable these inputs. We also aim to assess the way in which landscape features in CGSM such as artificial channels and roads may affect the hydrologic connectivity of the wetland and threaten its sustainability. Unfortunately, due to its remoteness and spatial extension, the wetland lacks a hydrologic monitoring network. Hence, we employ Wetland Interferometric Synthetic Aperture Radar (Wetland InSAR), a technology based on remote sensing, to detect large-scale water level changes in time and space. We combine the results obtained from wetland InSAR with a hydrologic analysis of water levels and water discharge in the main tributary river to study the hydrologic connectivity of the wetland. We further suggest general guidelines for the improvement of the CGSM's hydrologic connectivity.

2. Methods

2.1. Study area

The CGSM comprises four large water bodies: the Main Lagoon, Salamanca island mangrove forest, located close to the city of Barranquilla, and the Northern and Southern Pajarales complexes located between the Main Lagoon and the Magdalena River (figure 1). Mangrove mortality is mostly concentrated in the Northern Pajarales complex. The Pajarales complex receives water from the Magdalena River, located west of the complex, through a series of natural and artificial channels among which Renegado, Aguas Negras, El Salado, and New Clarin Channels are the most significant. Flow regulation for agriculture and heavy siltation of the natural channels that feed the CGSM from the Magdalena River appear to restrict fresh water inputs into the CGSM and hamper river-to-wetland connectivity.

The annual precipitation over the CGSM experiences a bimodal seasonality of two dry seasons (roughly from December to April and July to August) and two wet seasons (roughly May to June and September to November); further, it is higher in the wet South (1330 mm yr^{-1}) in comparison to the dry North (870 mm yr^{-1}). The opposite takes place with potential evapotranspiration (2000 mm yr^{-1} and 500 mm yr^{-1}, respectively) (Blanco *et al* 2006). The arrival and duration of the season depends on whether the year is under El Niño or La Niña conditions. Pore water salinities are found within the range of 0 to 134 PSU.

2.2. Wetland InSAR

Common InSAR employs differences in the phase path length of two satellite acquisitions taken from the same orbital position, at the same resolution, and over the same region, to generate displacement maps representing the changes in the solid surface over time (Wdowinski *et al* 2004). These maps are referred to as interferograms and include visualization of phase differences indicated by coloration, and at times, contain shaky contour lines known as 'fringes', which can be either continuous or discontinuous (Ferretti *et al* 2007). Instead, Wetland InSAR can generate displacement maps of the water surface that have been previously employed to detect water movements in wetlands (Hong *et al* 2010, Kim *et al* 2009, Kim *et al* 2013, Lu and Kwoun 2008, Oliver-Cabrera and Wdowinski 2016, Gondwe *et al* 2010, Xie *et al* 2013, Lu *et al* 2009).

In this study, we obtained 29 ALOS-PALSAR satellite images from the Alaska Satellite Facility web portal, taken between the years 2007 and 2011 and covering the two scenes in the area of the CGSM (figure 1). We generated 66 interferograms (25 for Scene 1 and 41 for Scene 2, respectively) through selection of pairs of images with less than 365 days of gap between them, since differential interferograms over wetlands have low coherence beyond these thresholds (see supplementary materials and figure S1 available at stacks.iop.org/ERL/13/024003/mmedia). Coherence constitutes a unitless measure of the correlation between the two interferometric acquisitions that ranges from 0 (low) to 1 (high). The higher the coherence of an interferogram, the more possible it is to recognize a fringe pattern for water level change. We studied each interferogram to identify continuous and discontinuous fringe patterns that represent changes in water level difference between the two acquisitions. While continuous fringe patterns represent wetland water flow, discontinuous fringes or sharp phase changes represent a lack of connectivity between areas on both sides of the discontinuity. We analyzed the most persistent fringe patterns across the interferograms obtained from the Wetland InSAR technology

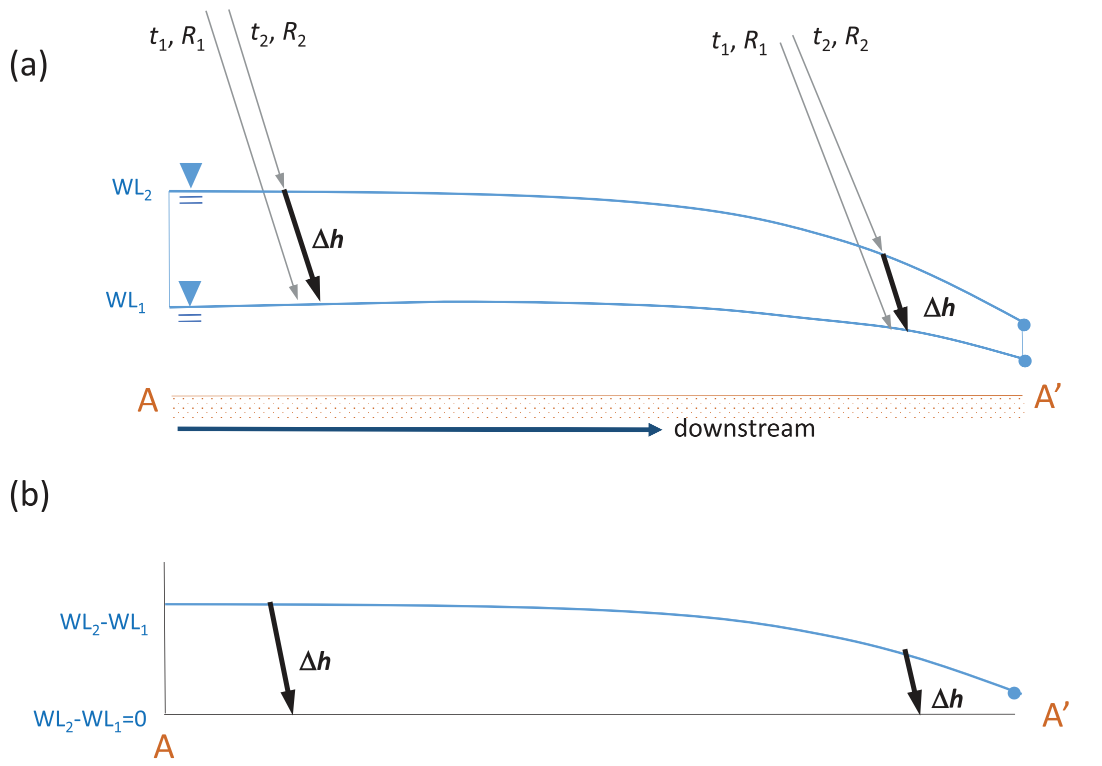

Figure 2. Conceptual model representing the satellite path length (phase) changes linked to water level changes along a wetland transect, where the predominant radar backscattering signal is a water/vegetation double bounce reflection. (*a*) Phase differences along the line of sight between two images (R_1, R_2) taken at different times (t_1, t_2) along a given transect in the wetland's downstream direction (A-A'). Reference point is A'. (*b*) The difference in water level between the two satellite acquisitions ($\Delta h = \mathrm{WL}_1 – \mathrm{WL}_2$) can be approximated from the difference in phase of the two satellite paths (see equation (1) in supplementary materials). The illustrated diagram corresponds to a hypothetical water profile difference when the daily discharge in the Magdalena River during the first acquisition (Q_1) is lower than in the second (Q_2) and under similar tide conditions.

and attempted to relate them to water change and wetland hydrodynamics.

2.3. Relating wetland water level changes and Magdalena river discharge

The InSAR-derived water level change observations are relative in time and space. Over time, the observed changes represent water level changes between two acquisition dates (figure 2). In space, the measurements are in relation to a point of reference (e.g. point A' in figure 2). As we set the reference point in a hypothetical stable area with small water level changes, the observed measurements reflect the difference in water level between the two acquisition dates. Under natural conditions, water levels in each acquisition date (WL1, WL2) should relate to water changes in Magdalena River discharge during that acquisition (Q_1, Q_2) as the CGSM forms a part of the Magdalena River Delta. To determine if this is the case even after the large hydrologic modifications suffered by the CGSM, we calculated the difference in mean daily discharge between the two acquisition dates ($\Delta Q = Q_2 – Q_1$) at the nearest discharge station on the Magdalena River, located 30 km upstream of the mouth of the Renegado Channel (figure 1(*a*)). For the sake of the multi-interferogram hydrologic analysis, we constructed the interferograms in such a way that the phase value from the acquisition date with the highest daily discharge Q (of the two dates) was subtracted from that of the lowest discharge. i.e. $\Delta Q > 0$. Under the assumption that changes in the Magdalena River reflect differences in water level between the two satellite acquisitions, the difference in water level between acquisitions under similar tide conditions ($\Delta h = \mathrm{WL}_1 – \mathrm{WL}_2$) is expected to be positive and decreasing in the downstream direction (figure 2), following the typical profile of a riverine water discharge into an estuary (see Cai *et al* 2016 and Bolla Pittaluga *et al* 2015).

We selected transects for the two regions where the most persistent continuous fringes occurred (figure 3) and extracted the wrapped phase change ($\Delta\Phi$) for all pixels in the interferogram that were intersected by these transects. The wrapped phase changes are expressed in the range from 0 to 2π. We unwrapped the phase change, calculated the magnitude of the corresponding change in water level, and repeated this procedure for all coherent interferograms (see supplementary materials).

3. Results

3.1. Fresh water inputs

We conducted a hydrologic analysis of the interferograms in order to detect the degree of connectivity

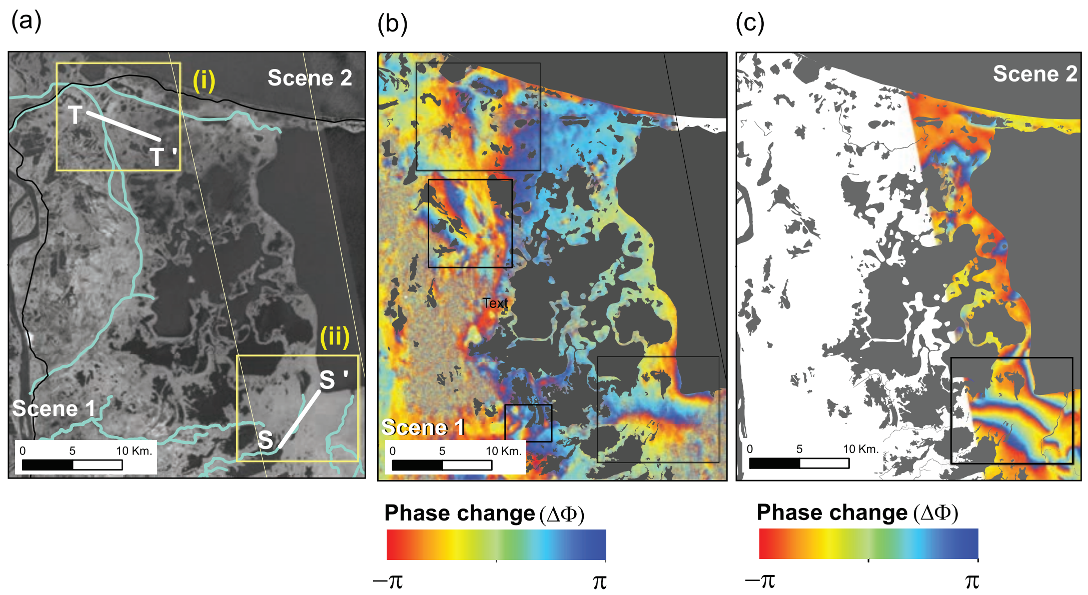

Figure 3. Interferogram of phase (water level) changes under wet conditions. (*a*) Example image of the Pajarales complex of the CGSM study area (figure 1), with regions of persistent fringe patterns (yellow and black rectangles (i) and (ii)) and corresponding transects (T-T' and S-S', white) used to study the water level changes and the role of channels (blue) as fresh water inputs. Wrapped interferograms of phase change ($\Delta\Phi$) for (*b*) the acquisition pair of 2010/07/29 and 2010/10/29 (Scene 1) and (*c*) the acquisition pair of 2010/08/27 and 2011/01/12 (Scene 2).

between the Magdalena River and the CGSM during the period of the acquisitions studied (2007–2011). The acquisition pairs of 2010/07/29 and 2010/10/29 (Scene 1) and acquisition pairs of 2010/08/27 and 2011/01/12 (Scene 2) were taken as representative of 'wet conditions' for each scene since they had the largest corresponding mean Q of all interferograms (i.e. $(Q_1 + Q_2)/2$). These pairs showed a mean Q of 856 $m^3\,s^{-1}$ and 847 $m^3\,s^{-1}$, and a ΔQ of 106 $m^3\,s^{-1}$ and 50 $m^3\,s^{-1}$, respectively (figures 3(*b*) and (*c*)). Two main regions of continuous fringes were identified: (i) along the wedged formed by the Marquez and New Clarín channels, signaling fresh water input through the New Clarín Channel and (ii) the mouth of the Renegado Channel in the Southern Pajarales. The shape of the two fringe patterns (figures 3(*b*) and (*c*)) and the fact that the phase change decreased in the downstream direction when $\Delta Q > 0$ inferred that the origin of the phase shift and the corresponding water level change was linked to fresh water inputs from the Magdalena River. A phase shift cycle of more than 2π (full colour range) could be identified in four out of 25 interferograms in (i) and 10 out of 41 in (ii). Although not as persistent among interferograms, two other regions showed marked fringe patterns in Scene 1: the flooding of the eastern plains from the Magdalena River but not exceeding beyond the Marquez Channel (south of (i)) and the mouth of the Salado Channel (west of (ii)) (figure 3(*b*)).

For the acquisition pairs of 2010/07/29 and 2010/10/29 (Scene 1), spatial unwrapping of the phase shift map along the line of sight of the satellite (figure 4(*a*–*c*)) and conversion to water height change (figure 4(*d*)) revealed a water level difference profile that decreased along the transects T-T' and S-S'. The total accumulated water level difference (Δh_{acc}) in each transect was −18 and −20 cm, respectively. Nevertheless, different hydraulic processes appear to occur in these two regions based on the differences in curvature of the Δh profile along the two transects.

For the purpose of comparison, we also analyzed the interferogram with the lowest corresponding mean Q (mean $Q = 557\ m^3\,s^{-1}$ and $\Delta Q = 33\ m^3\,s^{-1}$) indicative of 'dry conditions' (figure 5 and S2). Although the interferogram presented high coherence, it did not exhibit continuous fringes such as those observed in the wet interferogram. During the dry season, levels in the Magdalena River drop considerably, to the point that fresh water inputs from this source into the CGSM appear to be negligible. The phase changes along the two transects S-S' and T-T' were found to be much less variable and did not complete a full phase change (i.e. $< 2\pi$). When the phase changes along the two transects S-S' and T-T' were unwrapped (figure 5), phase difference profiles along the transects fell below 6 cm and did not present a particular trend that would suggest a constant fresh water input. Hence, under these hydrologic conditions, there appeared to be no important fresh water input from the Magdalena River via New Clarín, Salado, and Renegado Channels into the CGSM. However, since the transect T-T' is closer to the sea than the transect S-S', the influence of tide on the water level should be greater in the former transect under these 'dry conditions'. Indeed, the maximum water level difference in the transect near the sea T-T' (6 cm) doubles in comparison to that of S-S' (3 cm) (figure 5(*d*)), suggesting stronger tidal influence near the coast.

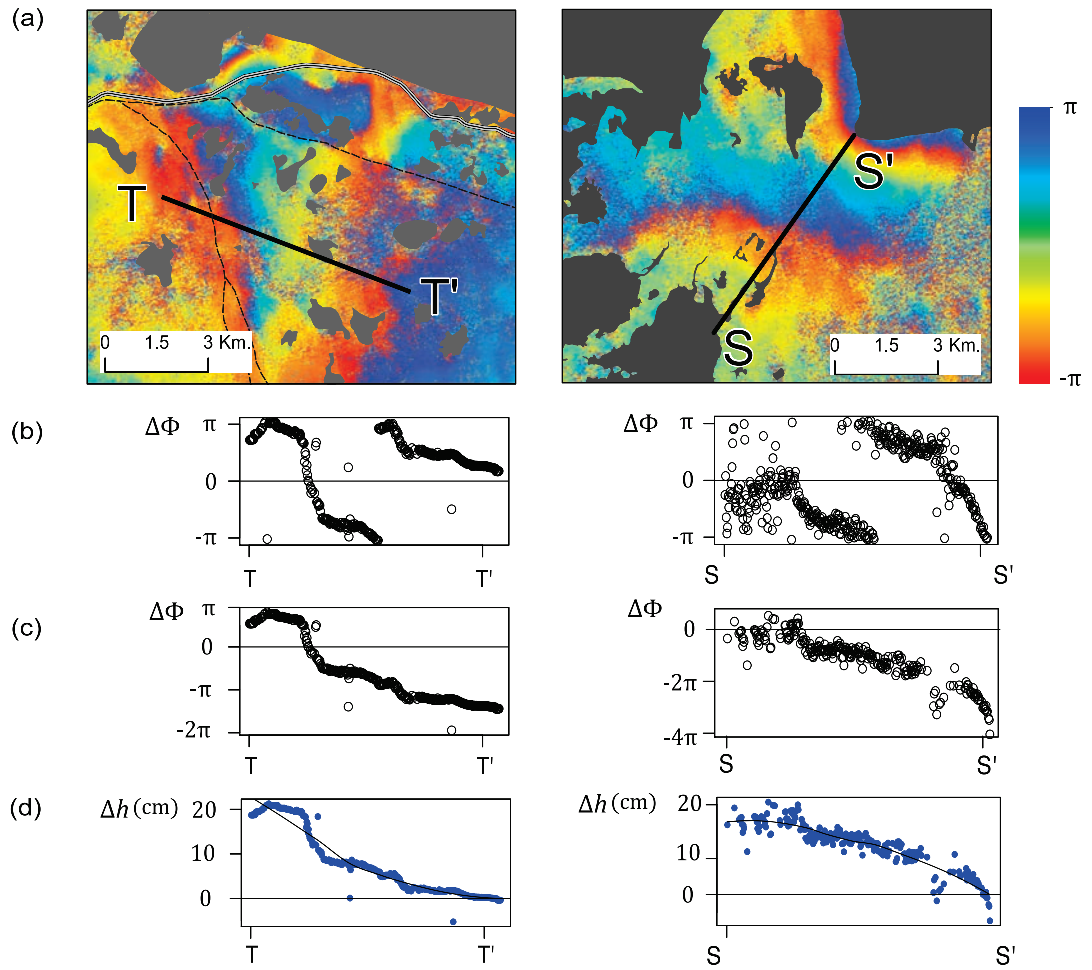

Figure 4. Profiles of water level change along transects in wet conditions. (*a*) Zoom to regions (i) and (iv) of figure 3 to see the acquisition pair of 2010/07/29 and 2010/10/29 (Scene 1) showing the locations of transects S-S' and T-T'. Reference points are S' and T', respectively. (*b*) Wrapped and (*c*) unwrapped phase change ($\Delta\Phi$) along the transects and (*d*) equivalent water level difference between the two acquisition dates (Δh) in centimeters are represented here.

However, in some interferograms even under 'wet conditions', observed water level change along the transect S-S' increases contrary to expected from fresh water inputs from the Magdalena River (see figure S3 for an example case). In this case, the extremely high accumulated water level difference (Δh_{acc} = 25 cm) can neither be explained through tide, since tidal daily water level differences as far as the transect S-S' have not been found to exceed 6 cm (figure S4). Rather, this case forms evidence of additional anthropogenic factors that control or alter the natural incoming of fresh water by regulation. In the case of the Renegado channel, the sluice gate that controls the flow at the mouth of the river may provide such a signal, as water does not enter the CGSM when the discharge is high due to flow control.

Using all available interferograms from both scenes yielded a statistically significant ($p < 0.05$) emerging relationship between ΔQ and Δh_{acc} along the transect S-S' (figure 6(*a*)). However, the ΔQ merely explained 17% of the variability observed in Δh_{acc}, probably due to the additional influence of tide and flow regulation. For all interferograms with large ΔQ (i.e. $\Delta Q > 200\, m^3\, s^{-1}$), Δh_{acc} was found to be negative, implying a profile of decreasing water level difference between the two acquisitions in the downstream direction (as in figures 2 and 4). Evidence of fresh water inputs along the Renegado Channel was further confirmed in the analysis of the maximum discharge of the two acquisitions for each interferogram (Q_{max}; figure 6(*b*)); fresh water inputs into CGSM mainly occurred when Q exceeded $700\, m^3\, s^{-1}$. The cumulative probability distribution of Q at Calamar station reveals that $700\, m^3\, s^{-1}$ is reached or passed only on 30% of the days during the period 2007–2011 (figure S5).

A similar analysis for transect T-T' at the mouth of the New Clarin Channel into CGSM displays no significant relationship between Δh_{acc} and ΔQ or Q_{max} (figure S6). Although this may evidence the hydrologic dysfunction of the channel due to sediment blockage, it may as well relate to the fact that only 11 coherent interferograms were available to determine the existence of such a relationship.

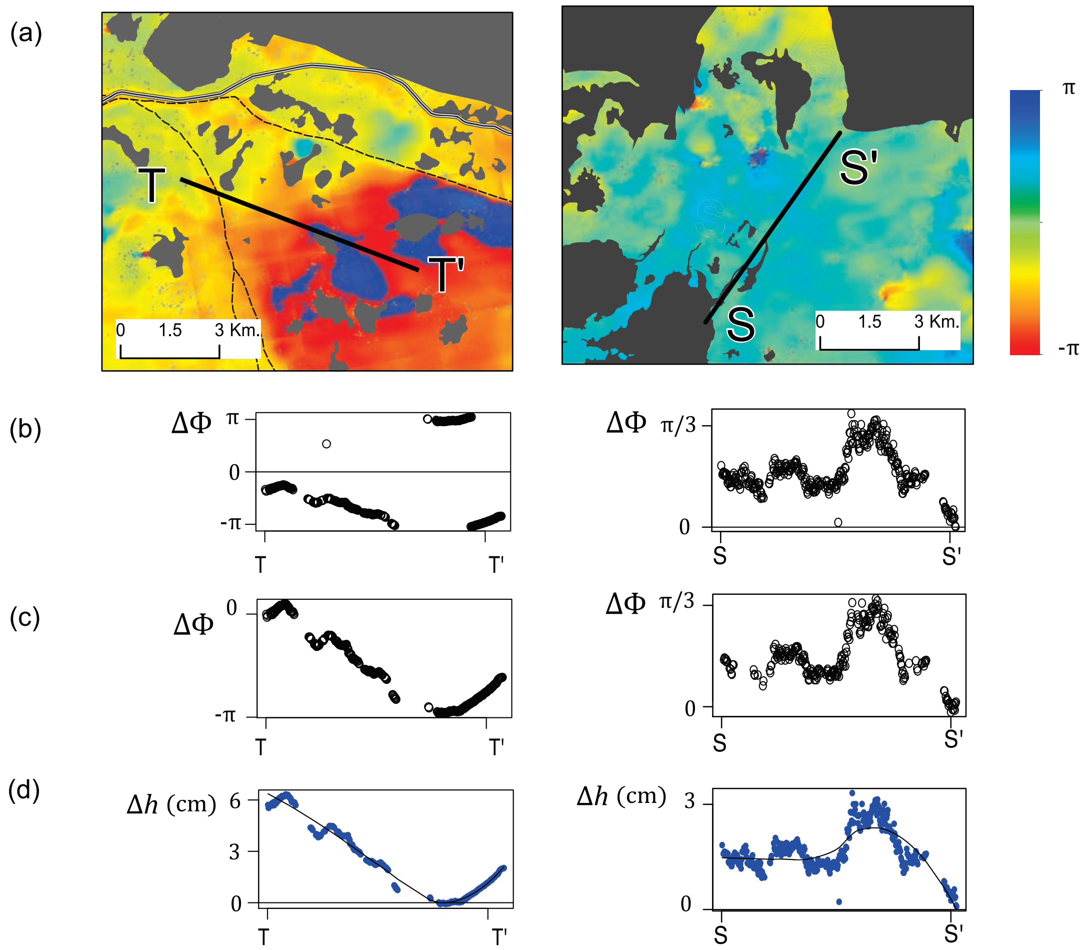

Figure 5. Profiles of water level changes along transects in dry conditions. (*a*) Zoom to regions (i) and (ii) of figure 3 to observe the acquisition pair of 2009/07/26 and 2009/09/10 (Scene 1) that depicts transects S-S' and T-T', the corresponding phase difference ($\Delta\Phi$) and water level change (Δh) in centimeters as shown in figure 4. The complete interferogram is revealed in supplementary figure S2.

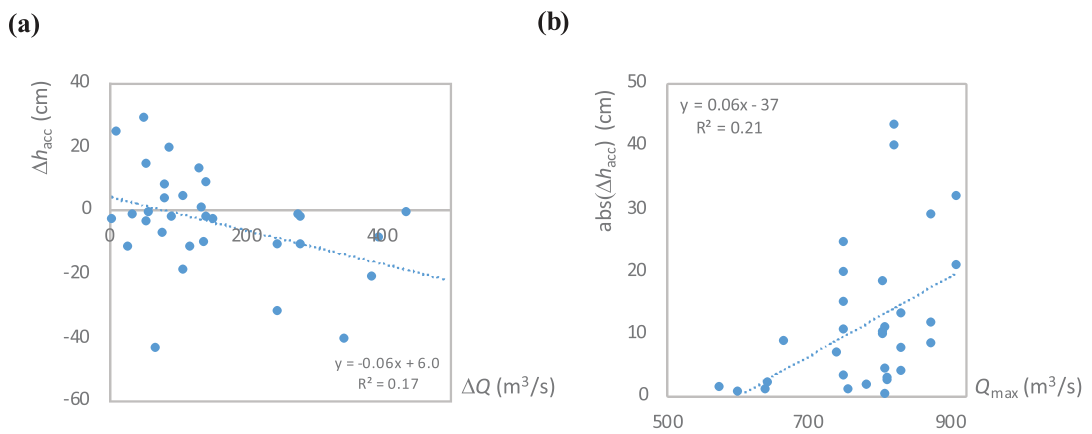

Figure 6. Relationship between water level change in the CGSM and water discharge in the Magdalena River. For the 32 interferograms that reveal coherence in the area of the transect S-S', (*a*) change in total water level difference along transect (Δh_{acc}) against difference in mean daily discharge between the two acquisitions (ΔQ). (*b*) Relationship between the absolute value of Δh_{acc} and the higher of the two mean daily discharge values corresponding to the two acquisition days (Q_{max}).

3.2. Impairment of hydrologic connectivity within CGSM

Both interferograms spanning over wet and dry conditions demonstrate discontinuous fringe patterns in particular in the Northern sector of CGSM that may represent barriers to hydrologic connectivity within the CGSM. In 15 out of 25 interferograms, abrupt changes in water level difference occur at both sides of the New Clarín Channel and can be observed along 10 km, suggesting low water connectivity between

Figure 7. Sediment barriers to hydrologic connectivity. Sediment accumulated along the banks of the artificial channels that act as a barrier to fresh water input into neighboring wetland bodies.

wetlands on both sides of this channel (figures 3(*b*), 4(*a*) and 5(*a*)). Similarly, judging through the long discontinuous fringe, the Marquez channel also isolates water bodies on both sides of its course, interrupting the flood plain sheet flow from the Magdalena River at least during dry conditions. Interestingly, the interrupting effect of these channels appears to be stronger than the isolating effect of the road that connects Barranquilla and Ciénaga since the road-related fringe discontinuity is not as frequent in the interferograms.

4. Discussion

The CGSM faces major siltation and hydrologic connectivity loss issues threatening its sustainability. To support its management and propose adequate solutions, it is of major importance to improve our understanding of the factors that lead to increased siltation and hypersaline conditions. The persistent fringes of water level difference along the New Clarín, Renegado, and Salado Channels suggest the provision of fresh water to the CGSM from the Magdalena River. Fresh water enters the CGSM, at least during the period of available satellite imagery, despite the construction of the road along the river's eastern bank, the flow control of the sluice gate at the entrance of the Renegado channel and the impairment of the channels due to heavy siltation.

It can be argued that channel-reopening operations have indeed allowed once again fresh water entry from the river. This may be related to the gradual recovery of mangrove within the wetland during the last two decades, as hypersalinity episodes are reduced due to availability of fresh water and salt dilution. Our results show that the Magdalena River supplies fresh water to the CGSM through the Renegado channel when discharge at Calamar station is above 700 m^3 s^{-1}. This conclusion is supported by observing accumulative phase change along the two transects: all the phase changes greater than 2π (> 15 cm of water height) occurred in interferograms in which at least one acquisition was taken when the Magdalena discharge at Calamar station was above 700 m^3 s^{-1}. However, based on the mediocre recovery of mangrove populations observed to date (INVEMAR 2016), 700 m^3 s^{-1} may be too high a quantity to allow fresh water inputs during dry conditions. A possible solution could be to introduce environmental restrictions to the sluice gate located at the mouth of the Renegado channel to guarantee minimum environmental flows.

In the case of the CGSM, wetland features that are supposed to enhance hydrologic connectivity (such as artificial channels) actually exhibit the opposite effect. In the New Clarín Channel, dredging operations that remove sediment deposits from the channel bed and settle them along the channels' banks actually isolate the water passing along the channel from its surroundings. This practice has been recurrent during the rehabilitation program of the CGSM (figure 7). The isolating effect is even more noticeable during dry periods when no fresh water entering from the Magdalena can pass the artificial sediment barriers along the channels. This may be one of the reasons to which mangroves along the wetlands on both sides of the New Clarín channel still suffer from hypersalinity events and have not recovered (INVEMAR 2016). It is then necessary to create openings within the accumulated sediment barriers along both banks of the artificial channels such as the New Clarín, in order to support fresh water entry into the neighboring wetlands.

5. Conclusions

Regarding the hydrologic connectivity between the CGSM and the Magdalena River, we found evidence of recent fresh water inputs despite the fact that the connectivity between the river and CGSM had been historically impaired through the construction of a road, the control of flow by a sluice gate, and the heavy siltation in the channels. We discovered a negative relationship between change in mean daily discharge between the two acquisition dates of the interferogram and the accumulative difference between water levels along a transect at the mouth of an important channel, establishing fresh water entry. However, fresh water inputs into CGSM through this channel mainly occurred when Q exceeded 700 $m^3 s^{-1}$, which corresponds to only 30% of the days during the period 2005–2014. The study also demonstrated the way in which artificial channels that are supposed to enhance hydrologic connectivity within the wetland actually result in the creation of barriers to water connectivity within CGSM. In order to increase the effectivity of the restoration project of the CGSM, we first recommend the introduction of environmental restrictions for the sluice gate located at the mouth of the Renegado channel to guarantee fresh water inputs under both dry and wet conditions. Second, we advise the construction of openings within the accumulated sediment barriers along both banks of the dredged artificial channels in order to support fresh water entry into the neighboring wetlands. This remote sensing based analysis of wetland connectivity can be replicated in other wetlands worldwide that suffer from a combination of hydrologic modifications, ecological degradation, and lack of hydrologic data.

Acknowledgments

The Swedish Research Council (VR, project 2009–3221) and the Swedish Research Council for Environment, Agricultural Sciences and Spatial Planning (942-2015-740) funded this study. We also acknowledge the application of satellite imagery from the Japan Aerospace Exploration Agency (JAXA) and the Alaska Satellite Facility (ASF) and the mangrove coverage maps to Jiner Bolaños of the Instituto de Investigaciones Marinas y Costeras de Colombia 'José Benito Vives de Andreis'—INVEMAR. We express gratitude towards the SARMAP team for their help and their efforts in continuous improvement of the SARScape InSAR processing toolbox. We also thank Lucia Licero for the photos that reports dredging operations in the CGSM. Partial support for VHRM's participation was provided by the Florida Coastal Everglades Long-Term Ecological Research program (grant nos DBI 0620409 and DEB-1237517). Finally, we thank the two anonymous reviewers for their suggestions and feedback, which have greatly improved this manuscript.

ORCID iDs

Fernando Jaramillo https://orcid.org/0000-0002-6769-0136

References

Barreto M B 2008 Diagnostics about the state of mangroves in Venezuela: case studies from the national park morrocoy and wildlife refuge care *Mangroves and Halophytes: Restoration and Utilisation Tasks for Vegetation Sciences* ed P H Lieth, D M G Sucre and B Herzog (Netherlands: Springer) pp 51–64

Blanco J, Viloria E and Narvaez J 2006 ENSO and salinity changes in the Cienaga Grande de Santa Marta coastal lagoon system, Colombian Caribbean *Estuar. Coast. Shelf Sci.* **66** 157–67

Bolla Pittaluga M, Tambroni N, Canestrelli A, Slingerland R, Lanzoni S and Seminara G 2015 Where river and tide meet: the morphodynamic equilibrium of alluvial estuaries *J. Geophys. Res. Earth Surf.* **120** 75–94

Botero L and Salzwedel H 1999 Rehabilitation of the cienaga grande de Santa Marta, a mangrove-estuarine system in the Caribbean coast of Colombia *Ocean Coast. Manage.* **42** 243–56

Cai H, Savenije H H G, Jiang C, Zhao L and Yang Q 2016 Analytical approach for determining the mean water level profile in an estuary with substantial fresh water discharge *Hydrol. Earth Syst. Sci.* **20** 1177–95

Cardona P and Botero L 1998 Soil characteristics and vegetation structure in a heavily deteriorated mangrove forest in the Caribbean coast of Colombia *Biotropica* **30** 24–34

Cintron G, Lugo A E, Pool D J and Morris G 1978 Mangroves of arid environments in Puerto Rico and adjacent Islands *Biotropica* **10** 110–21

Cohen M J *et al* 2016 Do geographically isolated wetlands influence landscape functions? *Proc. Natl Acad. Sci.* **113** 1978–86

Ferretti A, Monti-Guarnieri A, Prati C and Rocca F 2007 *InSAR Principles: Guidelines for SAR Interferometry Processing and Interpretation* (Netherlands: European Space Agency)

Flowers T J and Yeo A R 1986 Ion relations of plants under drought and salinity *Funct. Plant Biol.* **13** 75–91

Foti R, del Jesus M, Rinaldo A and Rodriguez-Iturbe I 2012 Hydroperiod regime controls the organization of plant species in wetlands *Proc. Natl Acad. Sci.* **109** 19596–600

Freeman M C, Pringle C M and Jackson C R 2007 Hydrologic connectivity and the contribution of stream headwaters to ecological integrity at regional scales *J. Am. Water Resour. Assoc.* **43** 5–14

Golden H E, Lane C R, Amatya D M, Bandilla K W, Raanan Kiperwas H, Knightes C D and Ssegane H 2014 Hydrologic connectivity between geographically isolated wetlands and surface water systems: a review of select modeling methods *Environ. Model. Softw.* **53** 190–206

Gondwe B R N, Hong S-H, Wdowinski S and Bauer-Gottwein P 2010 Hydrologic dynamics of the ground-water-dependent Sian Ka'an Wetlands, Mexico, derived from InSAR and SAR data *Wetlands* **30** 1–13

Hong S-H, Wdowinski S, Kim S-W and Won J-S 2010 Multi-temporal monitoring of wetland water levels in the florida everglades using interferometric synthetic aperture radar (InSAR) *Remote Sens. Environ.* **114** 2436–47

INVEMAR 2015 Monitoreo de las condiciones ambientales y los cambios estructurales y funcionales de las comunidades vegetales y de los recursos pesqueros durante la rehabilitación de la Ciénaga Grande de Santa Marta *Informe Técnico.* **14** 1–188

Jaramillo F and Destouni G 2015 Local flow regulation and irrigation raise global human water consumption and footprint *Science* **350** 1248–51

Jimenez J A, Lugo A E and Cintron G 1985 Tree mortality in mangrove forests *Biotropica* **17** 177–85

Kim J-W, Lu Z, Lee H, Shum C K, Swarzenski C M, Doyle T W and Baek S-H 2009 Integrated analysis of PALSAR/Radarsat-1 InSAR and ENVISAT altimeter data for mapping of absolute water level changes in Louisiana wetlands *Remote Sens. Environ.* **113** 2356–65

Kim S W, Wdowinski S, Amelung F, Dixon T H and Won J S 2013 Interferometric coherence analysis of the Everglades wetlands, South Florida *IEEE Trans. Geosci. Remote Sens.* **51** 5210–24

Krauss K W, Lovelock C E, McKee K L, López-Hoffman L, Ewe S M L and Sousa W P 2008 Environmental drivers in mangrove establishment and early development: a review *Aquat. Bot.* **89** 105–27

Lu Z, Kim J-W, Lee H, Shum C K, Duan J, Ibaraki M, Akyilmaz O and Read C-H 2009 Helmand river hydrologic studies using ALOS PALSAR InSAR and ENVISAT altimetry *Mar. Geod.* **32** 320–33

Lu Z and Kwoun O I 2008 Radarsat-1 and ERS InSAR analysis over southeastern coastal Louisiana: implications for mapping water-level changes beneath swamp forests *IEEE Trans. Geosci. Remote Sens.* **46** 2167–84

Martínez G A R 2005 Ciénaga Grande de Santa Marta—un modelo de gestión interinstitucional para su recuperación. CORPAMAG

Oliver-Cabrera T and Wdowinski S 2016 InSAR-based mapping of tidal inundation extent and amplitude in Louisiana coastal Wetlands *Remote Sens.* **8** 393

Osland M J, Enwright N M, Day R H, Gabler C A, Stagg C L and Grace J B 2016 Beyond just sea-level rise: considering macroclimatic drivers within coastal wetland vulnerability assessments to climate change *Glob. Change Biol.* **22** 1–11

Polidoro B A *et al* 2010 The loss of species: mangrove extinction risk and geographic areas of global concern *PLoS ONE* **5** e10095

Pringle C M 2001 Hydrologic connectivity and the management of biological reserves: a global perspective *Ecol. Appl.* **11** 981–98

Quin A, Jaramillo F and Destouni G 2015 Dissecting the ecosystem service of large-scale pollutant retention: the role of wetlands and other landscape features *AMBIO* **44** 127–37

Rivera-Monroy V H *et al* 2011 Salinity and chlorophyll a as performance measures to rehabilitate a mangrove-dominated deltaic coastal region: the Cienaga Grande de Santa Marta-Pajarales Lagoon Complex, Colombia RID G-7329-2011 *Estuaries Coasts* **34** 1–19

Thorslund J *et al* 2017 Wetlands as large-scale nature-based solutions: status and challenges for research, engineering and management *Ecol. Eng.* **108** 489–497

Van Meter K J and Basu N B 2015 Signatures of human impact: size distributions and spatial organization of wetlands in the Prairie Pothole landscape *Ecol. Appl.* **25** 451–65

Wdowinski S, Amelung F, Miralles-Wilhelm F, Dixon T H and Carande R 2004 Space-based measurements of sheet-flow characteristics in the Everglades wetland, Florida *Geophys. Res. Lett.* **31** L15503

Wemple B C *et al* 2017 Ecohydrological disturbances associated with roads: current knowledge, research needs, and management concerns with reference to the tropics *Ecohydrology* e1881

Xie C, Shao Y, Xu J, Wan Z and Fang L 2013 Analysis of ALOS PALSAR InSAR data for mapping water level changes in Yellow River Delta wetlands *Int. J. Remote Sens.* **34** 2047–56